

# Part-per-trillion level SF<sub>6</sub> detection using a quartz enhanced photoacoustic spectroscopy-based sensor with single-mode fiber-coupled quantum cascade laser excitation

Vincenzo Spagnolo,<sup>1,\*</sup> Pietro Patimisco,<sup>1</sup> Simone Borri,<sup>1</sup> Gaetano Scarmacio,<sup>1</sup>  
Bruce E. Bernacki,<sup>2</sup> and Jason Kriesel<sup>3</sup>

<sup>1</sup>Dipartimento Interateneo di Fisica, University and Politecnico of Bari, CNR-IFN UOS BARI, Via Amendola 173, Bari 70100, Italy

<sup>2</sup>Pacific Northwest National Laboratory, 902 Battelle Boulevard, Richland, Washington 99354, USA

<sup>3</sup>Opto-Knowledge Systems Inc., 19805 Hamilton Avenue, Torrance, California 90502, USA

\*Corresponding author: spagnolo@fisica.uniba.it

Received August 28, 2012; revised September 19, 2012; accepted September 21, 2012;  
posted September 21, 2012 (Doc. ID 175153); published October 23, 2012

A sensitive spectroscopic sensor based on a hollow-core fiber-coupled quantum cascade laser (QCL) emitting at 10.54  $\mu\text{m}$  and quartz enhanced photoacoustic spectroscopy (QEPAS) technique is reported. The design and realization of mid-IR fiber and coupler optics has ensured single-mode QCL beam delivery to the QEPAS sensor. The collimation optics was designed to produce a laser beam of significantly reduced beam size and waist so as to prevent illumination of the quartz tuning fork and microresonator tubes. SF<sub>6</sub> was selected as the target gas. A minimum detection sensitivity of 50 parts per trillion in 1 s was achieved with a QCL power of 18 mW, corresponding to a normalized noise-equivalent absorption of  $2.7 \times 10^{-10} \text{ W} \cdot \text{cm}^{-1} / \text{Hz}^{1/2}$ . © 2012 Optical Society of America  
OCIS codes: 280.3420, 140.5960.

The detection and quantification of trace chemical species in the gas phase is of considerable interest in a wide range of applications such as industrial process monitoring, noninvasive industrial inspection, etc. The use of spectroscopic analysis based on mid-IR sources are attracting a great interest thanks to their inherent high sensitivity and selectivity. Quantum cascade lasers (QCLs) can have a strong impact in these fields because of their wavelength agility, portability, robustness, and power [1]. In combination with QCLs, quartz enhanced photoacoustic spectroscopy (QEPAS) offers the advantage of high sensitivity and fast time-response. Very efficient QCL-based QEPAS sensors have been demonstrated for trace detection of several chemical species, such as NH<sub>3</sub>, NO, CO<sub>2</sub>, N<sub>2</sub>O, CO, CH<sub>2</sub>O, C<sub>3</sub>H<sub>6</sub>O, etc. [1–8], as low as single part per billion concentration levels. Enhanced versatility of such sensor systems can be obtained via optical fiber delivery and coupling. Ultra compact QEPAS spectrophones [incorporating quartz tuning fork (QTF), acoustic resonator, and fiber focuser] have been realized employing fiber-coupled near-IR diode laser sources [9,10]. The feasibility to extend this approach also to mid-IR light sources will allow compact integration with QCLs. However, due to limited availability of mid-IR single mode fibers, the implementation of fiber-coupled-based QCL sensors has to our knowledge not previously been reported.

We report here the design and realization of QEPAS sensors based upon an external cavity (EC)-QCL laser source emitting at 10.54  $\mu\text{m}$ , fiber-coupled with a QEPAS spectrophone module. We selected sulphur hexafluoride (SF<sub>6</sub>) as the target gas molecule. SF<sub>6</sub> is an invisible, nonhazardous inert gas with near-perfect dielectric properties that is used as an insulating gas in high-voltage switch gear and circuit breakers. It is also an extremely efficient absorber of infrared radiation, making it one of

the most effective known greenhouse gases [11]. SF<sub>6</sub> has also been employed in leak detection systems since it is an inert gas [12].

The architecture of the QCL fiber-coupled QEPAS sensor is shown schematically in Fig. 1.

The sensor platform is based on a  $2f$  wavelength-modulation spectroscopy-based QEPAS-detection approach. A widely tunable continuous wave EC-QCL (Daylight Solutions, Inc., model 21106-MHF) served as the excitation source for generating the QEPAS signal. The laser optical frequency can be scanned over  $\sim 0.6 \text{ cm}^{-1}$  by applying a modulated voltage of up to 100 V at 1 Hz to a piezoelectric translator attached to the diffraction grating element of the EC-QCL. For higher

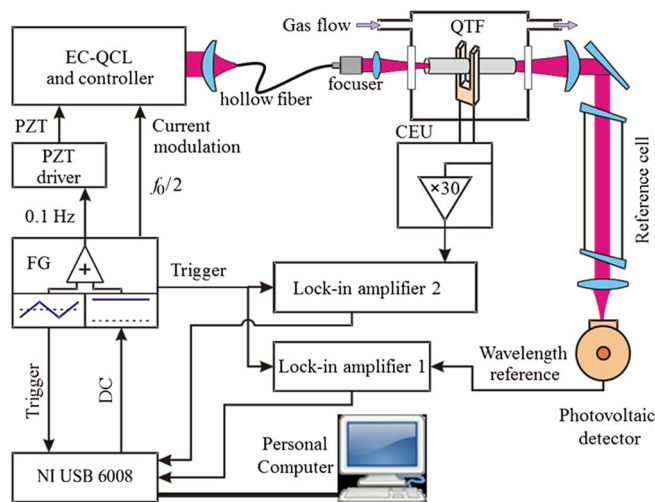


Fig. 1. (Color online) Schematic of QCL fiber-coupled QEPAS sensor. PZT, piezoelectric translator; QTF, quartz tuning fork; FG, dual channel function generator; and CEU, control electronics unit.

modulation frequency, an internal bias tee allows external modulation of the QCL current via an input voltage signal to obtain up to  $0.1 \text{ cm}^{-1}$  optical frequency modulation at 2 MHz. Wavelength modulation technique is implemented by applying a sinusoidal dither to the laser current at half of the QTF resonance frequency and detecting the QTF response at  $2f$  by means of a lock-in amplifier. The control electronics unit is used to determine the QTF parameters: dynamic resistance  $R$ , quality factor  $Q$ , and resonant frequency  $f_0$ . It is also used to pass on the 30 times amplified signal from a transimpedance amplifier to the lock-in amplifier. The lock-in amplifiers and a function generator (Tektronix model AFG3102) are controlled through a USB NI card, using LabVIEW-based software. The time constant of the lock-in amplifiers was set to 100 ms for all QEPAS measurements reported in this work. The related bandwidth is 1.6675 Hz. To further enhance the signal, a microresonator (mR) has been added to the QTF sensor architecture [10]. The mR consists of two metallic tubes with size (3.9 mm long and 0.84 mm inner diameter) optimized to maximize the signal-to-noise ratio (SNR) when using mid-IR lasers at low operating pressure (below 150 Torr) [7]. The light exiting the compact acoustic detection module (ADM) is directed into a reference channel consisting of a 10 cm long reference cell, filled with a 0.1%  $\text{SF}_6$  in  $\text{N}_2$ , and a photovoltaic detector (VIGO, PVI-3TE-6-1).

The third harmonic with respect to the laser modulation frequency of the VIGO signal serves as a spectral reference.

In QEPAS experiments it is critical to avoid laser illumination of the ADM system, since the radiation blocked by the mR or QTF results in an undesirable nonzero background when absorbed by the ADM structural elements. This background is usually several times larger than the thermal noise level of QEPAS and can carry a shifting fringe-like interference pattern, which strongly limits the detection sensitivity [7,13]. Thus it is important to employ a mid-IR QEPAS excitation beam of high quality and stability, and if employing a fiber coupling system, single mode beam delivery is required. For our sensor architecture we designed and realized a single mode QCL-QEPAS fiber coupling system. Single mode laser delivery has been obtained using a hollow fiber [14] with inner Ag-AgI coatings and an internal bore size of 300  $\mu\text{m}$ , having a loss of 1 dB/m. Additional collimating/focusing optics have been designed to be attached to the output of the fiber and provide a focusing distance of 38 mm. The resulting beam waist at the QTF has a diameter of  $\sim 160 \mu\text{m}$  with an energy that is  $\sim -20 \text{ dB}$  from the peak at the QTF prongs. For optimum alignment, 65% of the output laser power is transmitted through the complete optical system. An example of the single mode 2D

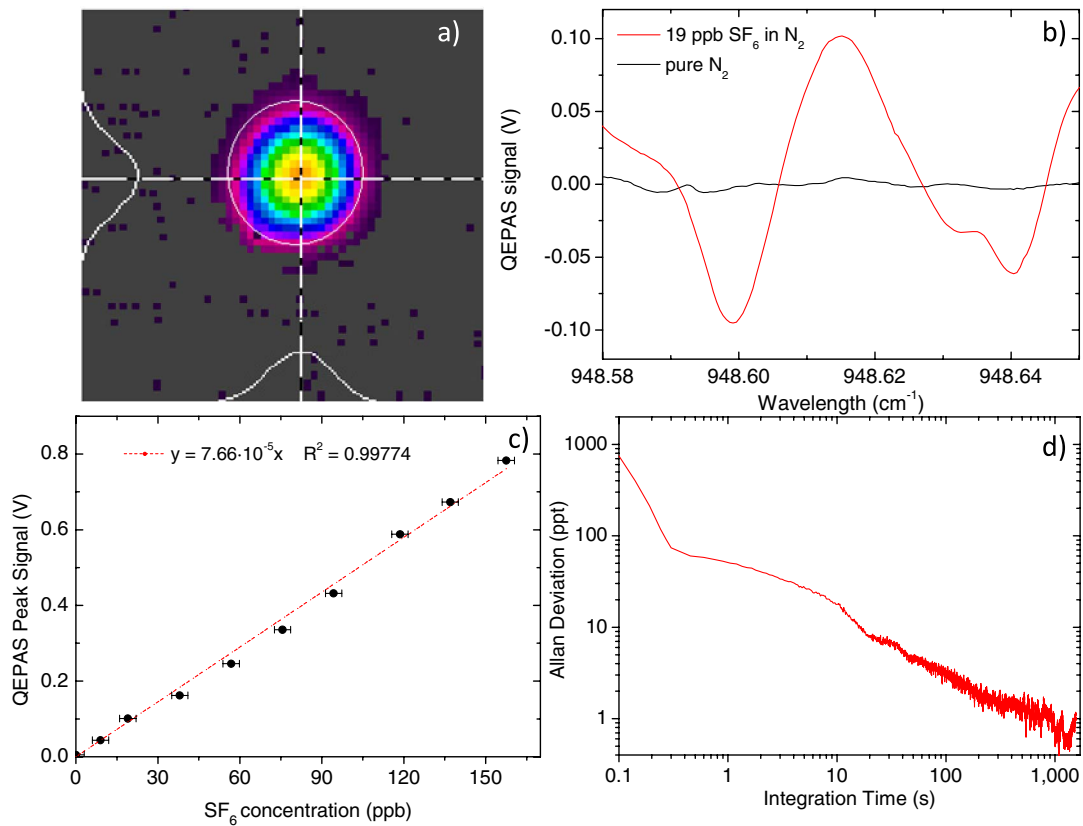


Fig. 2. (Color online) (a) Two-dimensional single mode profile of the EC-QCL beam exiting the hollow fiber, along with the related one-dimensional Gaussian-like profiles. (b) QEPAS spectra measured in a scan mode for a 19 ppb  $\text{SF}_6:\text{N}_2$  calibrated gas mixture and for pure  $\text{N}_2$ . The noise fluctuations in Fig. 2(b) are  $\sim 4 \text{ mV}$ . (c) QEPAS peak signal as a function of the  $\text{SF}_6$  concentration based on a calibration with a gas dilution system. The dashed line represents a linear fit of the data. The small deviations from the linear trend are partially due to uncertainty in the gas mixture concentration ( $< 3 \text{ ppb}$ ). (d) Allan deviation in parts per trillion (ppt) of the QEPAS signal as a function of the integration time. The rapid decrease from 0.1 to 0.3 s reflects delay and the related oscillations in the feedback loop when balancing the signal of the reference channel at low integration time ( $< 0.3 \text{ ms}$ ).

beam profile exiting from the fiber is shown in Fig. 2(a). In our experiments, 18 mW of optical laser power was focused into the ADM, and 99.4% of the laser beam coming out the collimator is transmitted through the ADM without touching it. The gap between the QTF prongs is  $\sim 300 \mu\text{m}$ .

For  $\text{SF}_6$  detection we selected the absorption band peaked at  $948.62 \text{ cm}^{-1}$  in the spectral region of the  $\nu_3$  fundamental band, which is characterized by several strong rotational-vibrational absorption lines separated by less than  $0.05 \text{ cm}^{-1}$ . Thus, in order to observe well resolved spectral absorption features, it is necessary to work at low-pressure conditions (i.e.,  $<100 \text{ Torr}$ ). Preliminary experiments were performed to study the QEPAS signal as a function of gas pressure and laser current modulation depth. A gas pressure of 75 Torr and modulation voltage of 4.2 Vpp correspond to the optimum condition in terms of signal and SNR [15].

In Fig. 2(b) is shown a spectral scan of a 19 ppb  $\text{SF}_6$  sample in  $\text{N}_2$  at 75 Torr, together with the spectrum measured for pure  $\text{N}_2$  sample. No fringe-like interference pattern was observed, and the corresponding detection limit results  $\sim 750 \text{ ppt}$ . The lack of clear zero signal off the  $\text{SF}_6$  feature in Fig. 2(b) is due to the presence of neighbors'  $\text{SF}_6$  absorption lines. Stepwise concentration measurements were performed to verify the linearity of the QEPAS signal as a function of the  $\text{SF}_6$  concentration. A trace gas standard generator is used to produce  $\text{SF}_6$  concentrations in the range 0–160 ppb, using  $\text{N}_2$  as the diluting gas. The system was operated in the locked mode, i.e., with the QCL frequency set to the center of the absorption line. In Fig. 2(c), the mean value of the QEPAS peak signal is plotted for different  $\text{SF}_6$  concentrations from 9 up to 160 ppb. Above a  $\text{SF}_6$  concentration of 160 ppb, the QEPAS signal saturates the lock-in amplifier. The experimental data can be easily fit with a linear slope, confirming the linearity of the system response to concentration. To determine the achievable sensitivity of the QEPAS sensor we performed an Allan variance analysis [16], measuring and averaging the QEPAS signal at zero  $\text{SF}_6$  concentration. The Allan plot is shown in Fig. 2(d). For a 1 s averaging time (i.e.,  $0.16675 \text{ Hz}$  bandwidth), we achieve a minimum detection sensitivity of 50 parts per trillion (ppt), corresponding to a normalized noise equivalent absorption coefficient of  $\text{NNEA} = 2.7 \times 10^{-10} \text{ cm}^{-1} \text{ W/Hz}^{1/2}$ , which represents a record

value for the QEPAS technique. Under these conditions, the expected QEPAS signal still results several time larger than the QTF thermal noise ( $\sim 6 \mu\text{V}$ ); thus the sensitivity of the sensor is a result of the good  $\text{SF}_6$  absorption cross-sections and its fast V-T relaxation and limited mostly by stability of the radiation-related background.

The authors acknowledge financial support from the Italian research projects: PON01\_02238 and PON02\_00675.

## References and Notes

1. R. F. Curl, F. Capasso, C. Gmachl, A. A. Kosterev, B. McManus, R. Lewicki, M. Pusharsky, G. Wysocki, and F. K. Tittel, *Chem. Phys. Lett.* **487**, 1 (2010).
2. R. Lewicki, G. Wysocki, A. A. Kosterev, and F. K. Tittel, *Opt. Express* **15**, 7357 (2007).
3. R. Lewicki, J. H. Doty III, R. F. Curl, F. K. Tittel, and G. Wysocki, *Proc. Natl. Acad. Sci. USA* **106**, 12587 (2009).
4. A. A. Kosterev, P. R. Buerki, L. Dong, M. Reed, T. Day, and F. K. Tittel, *Appl. Phys. B* **100**, 173 (2010).
5. A. A. Kosterev, F. K. Tittel, D. V. Serebryakov, A. L. Malinovsky, and I. V. Morozov, *Rev. Sci. Instrum.* **76**, 043105 (2005).
6. C. Bauer, U. Willer, and W. Schade, *Opt. Eng.* **49**, 111126 (2010).
7. L. Dong, V. Spagnolo, R. Lewicki, and F. K. Tittel, *Opt. Express* **19**, 24037 (2011).
8. L. Dong, R. Lewicki, K. Liu, P. R. Buerki, M. J. Weida, and F. K. Tittel, *Appl. Phys. B* **107**, 275 (2012).
9. S. Schilt, A. A. Kosterev, and F. K. Tittel, *Appl. Phys. B* **95**, 813 (2009).
10. L. Dong, A. A. Kosterev, D. Thomazy, and F. K. Tittel, *Appl. Phys. B* **100**, 627 (2010).
11. Inventory of U. S. Greenhouse Gas Emissions and Sinks: 1990/2008, U. S. Environmental Protection Agency, Washington, D.C., USA, April 2010.
12. E. Huang, D. R. Rowling, T. Whelan, and J. L. Spiesberger, *J. Acoust. Soc. Am.* **114**, 1926 (2003).
13. V. Spagnolo, A. A. Kosterev, L. Dong, R. Lewicki, and F. K. Tittel, *Appl. Phys. B* **100**, 125 (2010).
14. J. M. Kriesel, N. Gat, B. E. Bernacki, R. L. Erikson, B. D. Cannon, T. L. Myers, C. M. Bledt, and J. A. Harrington, *Proc. SPIE* **8018**, 80180V1 (2011).
15. Under these conditions the modulation width results  $0.07 \text{ cm}^{-1}$  and the physical parameters of the QTF are  $Q = 22200$ ;  $R = 54.7 \text{ k}\Omega$ ;  $f_0 = 32762.6 \text{ Hz}$ .
16. P. Werle, *Appl. Phys. B* **102**, 313 (2011).